International Journal of Recent Development in Engineering and Technology
Website: www.ijrdet.com (ISSN 2347-6435 (Online) Volume 15, Issue 03, March 2026)

Analysis of Heat and Mass Transfer in Modified Eyring-Powell Flow over a Rotating Surface

Patroba Makori[1], Johana Kibet Sigey[2], Moffat Chamuchi[3], Emily Kilel[4]

[1,2]*Department of Pure and Applied Mathematics, Jomo Kenyatta University of Agriculture and Technology*
[3]*Department of Pure and Applied Mathematics, Kirinyaga University, Kenya.*
[4]*Department of Food Science and Nutrition, Karatina University*

***Abstract*-- The Eyring-Powell fluid model is a non-Newtonian fluids model that describes the flow of fluids such as clay, paint and blood. Previous studies found contradictory results regarding its rheological characteristics. The Modified Eyring-Powell fluid model overcomes these disparities by adding a new parameter that distinguishes between shear-thinning and shear-thickening models. Although few studies have been conducted on heat transfer in Modified Eyring-Powell fluids, mass transfer properties remain relatively unexplored. This study develops and examines the governing partial differential equations (PDEs) for heat and mass transfer in the Modified Eyring Powell fluid. Similarity transformations are used to convert the PDEs into a system of nonlinear ordinary differential equations (ODEs). The Chebyshev-collocation method is adopted to generate approximate numerical solutions. The result shows that the velocity, temperature, and concentration of modified Eyring-Powell fluid reduced with increasing rotational force.**

Nomenclature

Variables and Parameters

Fc - Coriolis force
τ - shear stress
B_0 - Constant magnetic field strength
Ω - Coriolis force
u, v - velocity in x and y directions
α - thermal diffusivity
T, C - Temperature, Concentration
μ, ϑ - dynamic and kinematic viscosity
g - Acceleration due to gravity
ρ - density
K - dimensionless Coriolis force
η - dimensionless distance
M - Magnetic field parameter
S_c - Schmidt number
G_{rt}, G_{rs} - Grashof parameters
r - Chemical reaction parameter
Pr - Prandtl number
Cf - Skin friction
N_b, N_t - Brownian and thermophoretic parameters
Nu - Nusselt number
J - Joule heating parameter
DB - mass diffusivity

I. Introduction

The Eyring-Powell fluid model has gained prominence in the modelling of non-Newtonian fluids due to its solid theoretical foundation and mathematical robustness. Unlike empirical models such as the power-law or Bingham models, the Eyring-Powell model is derived from the theory of reaction rates developed (Oke and Mutuku, 2021), originally to explain molecular deformation under stress. It expresses the relationship between shear stress and strain rate using a hyperbolic sine function, which enables it to describe both Newtonian and non-Newtonian behaviours without introducing singularities at zero shear rates. The theory considers the forces required to break two bonds of differing strengths, where one is strong bond and the other is a weak bond (Abegunrin et al., 2017; Kumar and Srinivas, 2020). This theoretical foundation enhances the practical relevance and adaptability of the Eyring-Powell fluid model in practical applications. Mucus, moisturising lotion, hair gel, yoghurt, latex paint, and polymeric solutions are examples of fluid modelled by the Eyring-Powell fluid model (Patel and Timol, 2009; Siddiqui et al., 2014; Rahimi et al., 2017; Junaid et al., 2023). The Eyring-Powell model is particularly effective in capturing behaviours such as creep deformation under sustained stress. Due to these properties, Eyring-Powell fluids have found applications in a wide range of fields, including the formulation of cosmetic products and industrial paints, and in the processing of clay slips and industrial greases.

Oke et al. (2023) applied the Eyring-Powell model and demonstrated that increasing the fluid's non-Newtonian parameter led to significant alterations in the velocity and temperature profiles. However, the original Eyring Powell model, despite its advantages, was not sufficient to capture the all-fluid behaviours observed in industrial and biological fluids. To address this, recent studies have proposed modifications to the model.

Oke (2021) introduced an additional parameter to control the degree of deformation. This has given rise to what is known as the Modified Eyring-Powell (MEP) model. Oke (2022) introduced a generalisation of the Eyring-Powell model by incorporating a deformation parameter q to regulate whether the fluid behaves as a shear-thinning or shear-thickening fluid. Some recent studies on the modified Eyring-Powell fluid include Anjum et al. (2022) who considered the influence of activation energy on the flow of modified Eyring-Powell fluid. Khan (2023) studied the biocovection and nonlinear radiation, Junaid et al. (2023) included the magnetic dipole effect, and Anjum et al. (2023) considered the activation energy.

However, Oke (2021) noted that the Eyring-Powell fluid model is a generalisation of Newtonian fluids and the shear-dependent fluids (whether shear-thinning or shear thickening). They also noted that the intrinsic characteristics of the Eyring-Powell fluid to alternate between shear-thinning and shear-thickening properties under some certain conditions was not been captured in the constitutive equations for the Eyring-Powell fluids. The lack of definition for the dual nature of the model has led several authors to produce conflicting results in literature. Some studies reported that velocity increases with increasing Eyring-Powell fluid parameter while others reported a decrease in velocity with increasing Eyring-Powell fluid parameter. Oke (2021) developed a model called the Modified Eyring-Powell (MEP) fluid that explains the reason for the conflicting outcomes. The Modified Eyring-Powell was developed by updating the Eyring-Powell constitutive equations with a deformation parameter whose values determine the shear-dependent nature of the fluid. By incorporating the deformation parameter, the Modified Eyring-Powell model successfully unified the conflicting outcomes by emphasizing that the outcomes are only evidence that the Eyring-Powell fluid model can capture both the shear-thinning and the shear-thickening properties of the fluid.

The application of the modified Eyring-Powell fluid model to tea manufacture is motivated by the need for a rigorous theoretical description of the rheological and transport phenomena arising during mechanically intensive processing stages (Rathnayake et al., 2023). Operations such as rolling, curling, and drying (Aaqil et al., 2023) involve the interaction of partially macerated tea leaves and expressed juices with rotating surfaces, producing a heterogeneous, non-Newtonian medium whose flow behaviour cannot be adequately captured by classical Newtonian models.

The modified Eyring-Powell formulation provides a suitable model to describe shear-dependent viscosity, stress distribution, and coupled heat and mass transfer under rotational effects. The model offers a scientific basis for analyzing process efficiency, equipment performance, and thermal control mechanisms. Although its use in tea manufacture is presently conceptual, this theoretical approach paves way to extend advanced non-Newtonian flow modelling to agro-industrial processing systems with the aim of improving process understanding and optimization.

As a relatively new class of fluid model, studies on Modified Eyring-Powell have focused mostly on the heat transfer in the flow. In this study, a mass transfer is included along with the heat transfer process in the Modified Eyring Powell flow over a linearly stretching and rotating surface.

Coriolis force is one of the inertia forces that affect flows over a rotating surface (Koriko et al., 2020). According to Koriko et al. (2020), Coriolis force acts mutually perpendicular to the velocity vector, introducing a fictitious force that deflects the direction of motion. The effect becomes significant in the momentum and thermal boundary layers. Applications of Coriolis force can be found in geophysical and industrial systems where the rate of rotation of the surface is significant in relation to the acceleration of the fluid. Modelling of flows in turbine, rotating disk reactors, meteorological systems, and centrifugal filtration devices cannot be accurate unless Coriolis force are incorporated. The Coriolis force is driven by the rate rotation of the surface upon which the flow is happening. Increase in surface rotation means an increase in the Coriolis force and vice versa. Lou et al. (2022) studied the influence of Coriolis force on dusty micropolar fluid and found that the rate of microrotation distribution is proportional to the size of Coriolis force. Khan and Uddin (2023) considered the influence of Coriolis force on unsteady bio-flow.

From the ongoing, it has become clear that Eyring-Powell fluid is able to capture both the shear-thinning and shear-thickening behaviours of the non-Newtonian fluids. The modified Eyring-Powell delineates the shear thinning from the shear-thickening properties by introducing a deformation parameter. As a relatively new class of fluid, studies have focused on the heat transfer in Eyring-Powell fluid flow and no study has considered the concentration equation in the flow over a rotating surface. This study is therefore set to analyze the heat and mass transfer in the modified Eyring-Powell fluid.

International Journal of Recent Development in Engineering and Technology
Website: www.ijrdet.com (ISSN 2347-6435 (Online) Volume 15, Issue 03, March 2026)

II. Governing Equations

II.1 Modified Eyring-Powell Model

According to Oke and Mutuku (2021), the shear stress for an Eyring-Powell fluid is derived from the understanding that there is a need to break a weak bond and a strong bond. The total shear stress is

$$\tau = \mu\nabla\mathbf{u} + \frac{1}{B}\operatorname{arcsinh}\left(\frac{1}{E}\nabla\mathbf{u}\right). \quad (1)$$

The modified Eyring-Powell fluid introduced by Oke (2021) and emphasized in Oke (2022), was derived by incorporating the deformation parameter q on the shear stress relative to the weak bond so that the total shear stress is

$$\tau = \mu\nabla\mathbf{u} + \left[\frac{1}{B}\operatorname{arcsinh}\left(\frac{1}{E}\nabla\mathbf{u}\right)\right]^q. \quad (2)$$

The momentum equation for the Modified Eyring-Powell fluid can then be written as

$$\rho\left(u_1\frac{\partial u_1}{\partial x_1} + u_2\frac{\partial u_1}{\partial x_2}\right) = \mu\frac{\partial^2 u_1}{\partial x_2^2} + \frac{q}{(BE)^q}\left(1 - \frac{(q+2)}{6E^2}\left(\frac{\partial u_1}{\partial x_2}\right)^2\right)\left(\frac{\partial u_1}{\partial x_2}\right)^{q-1}\frac{\partial^2 u_1}{\partial x_2^2},$$
$$u_1\frac{\partial u_1}{\partial x_1} + u_2\frac{\partial u_1}{\partial x_2} = \frac{\mu}{\rho}\frac{\partial^2 u_1}{\partial x_2^2} + \frac{q}{\rho(BE)^q}\left(1 - \frac{(q+2)}{6E^2}\left(\frac{\partial u_1}{\partial x_2}\right)^2\right)\left(\frac{\partial u_1}{\partial x_2}\right)^{q-1}\frac{\partial^2 u_1}{\partial x_2^2}. \quad (3)$$

The flow of Modified Eyring-Powell fluids is considered in this study by incorporating the concentration equation in the equations derived by Oke (2022). The Modified Eyring-Powell fluid is treated as incompressible, so that it is assumed that the density does not vary during the flow process. Assume that turbulence is disregarded so that the flow remains steady and laminar. Furthermore, the no-slip condition is enforced at the boundary, indicating that the fluid velocity coincides with that of the surface. Figure (1) shows the configuration of the flow and the conditions at the wall.

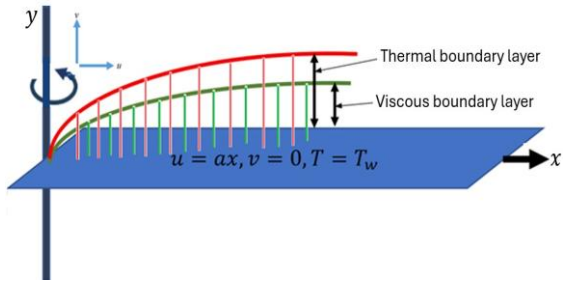

Figure I: Flow configuration

The equation governing the flow is the system of equations

$$\frac{\partial u_1}{\partial x_1} + \frac{\partial u_2}{\partial x_2} = 0, \quad (4)$$
$$u_1\frac{\partial u_1}{\partial x_1} + u_2\frac{\partial u_1}{\partial x_2} = \frac{\mu}{\rho}\frac{\partial^2 u_1}{\partial x_2^2} + \frac{q}{\rho(BE)^q}\left(1 - \frac{(q+2)}{6E^2}\left(\frac{\partial u_1}{\partial x_2}\right)^2\right)\left(\frac{\partial u_1}{\partial x_2}\right)^{q-1}\frac{\partial^2 u_1}{\partial x_2^2} - 2\Omega u_1, \quad (5)$$
$$u_1\frac{\partial T}{\partial x_1} + u_2\frac{\partial T}{\partial x_2} = \alpha\frac{\partial^2 T}{\partial x_2^2}, \quad (6)$$
$$u_1\frac{\partial C}{\partial x_1} + u_2\frac{\partial C}{\partial x_2} = D_B\frac{\partial^2 C}{\partial x_2^2}. \quad (7)$$

Conditions at the surface of the wall ($x_2 = 0$) obey the no-slip condition so that $u_1 = ax_1, C = C_w$, and $T = T_w$. Since the flow is not happening perpendicular to the surface, then $u_2 = 0$. By compiling these conditions, the conditions are

$$u_1 = ax_1,\ u_2 = 0,\ T = T_w,\ C = C_w, \text{ at } x_2 = 0, \quad (8)$$
$$u \to 0,\ T \to T_\infty,\ C \to C_\infty, \text{ as } y \to \infty. \quad (9)$$

2.2 Similarity Transformation

Consider the similarity variables chosen in Oke (2021) and Oke (2022) as

$$\eta = a1/2\vartheta - 1/2x_2, \quad (10)$$

with the stream function

$$\psi = a1/2\vartheta 1/2x1f. \quad (11)$$

To derive the expression for the variables u and v, we start by rewriting them as functions of the stream function such that

$$u_1 = ax_1\frac{df}{d\eta},\ u_2 = -a^{1/2}\vartheta^{1/2}f. \quad (12)$$

Furthermore, a rescaling transformation is given for T and C. Since $T \in [T_\infty, T_w]$ and $C \in [C_\infty, C_w]$, then they are transformed to the interval $[0,1]$ by the linear transformation

$$\Theta = \frac{T_w - T}{\Delta T},\ \Phi = \frac{C_w - C}{\Delta C}, \text{ where } \Delta C = C_w - C_\infty, \Delta T = T_w - T_\infty, \quad (13)$$

By using the variables (10) - (13), the dimensionless form of the equations (4) - (7) becomes

$$\left(1 + q\varepsilon\left(1 - \frac{(q+2)\delta^2}{3}\left(\frac{d^2 f}{d\eta^2}\right)^2\right)\left(\sqrt{2}\delta\frac{d^2 f}{d\eta^2}\right)^{q-1}\right)\frac{d^3 f}{d\eta^3} - K\frac{df}{d\eta} - \left(\frac{df}{d\eta}\right)^2 + f\frac{d^2 f}{d\eta^2} = 0, \quad (14)$$
$$\frac{d^2\Theta}{d\eta^2} + Prf\frac{d\Theta}{d\eta} = 0, \quad (15)$$
$$\frac{d^2\Phi}{d\eta^2} + Scf\frac{d\Phi}{d\eta} = 0, \quad (16)$$

,

International Journal of Recent Development in Engineering and Technology
Website: www.ijrdet.com (ISSN 2347-6435 (Online) Volume 15, Issue 03, March 2026)

and the dimensionless of the conditions (8)- (9) are

$$\frac{df}{d\eta}(0)=1,\ f(0)=0,\ \Theta(0)=0,\ \Phi(0)=0, \tag{17}$$

$$\frac{df}{d\eta}(\eta_\infty)=0,\ \Theta(\eta_\infty)=1,\ \Phi(\eta_\infty)=1. \tag{18}$$

where the parameters defined as

$$\delta^2=\frac{a^3x_1^2}{2\vartheta E^2},\ \varepsilon=\frac{1}{\mu BE},\ K=\frac{2\Omega}{a},\ \frac{\alpha}{\vartheta}=\frac{1}{Pr},\ \frac{D_B}{\vartheta}=\frac{1}{Sc}. \tag{19}$$

III. Solution Approach

3.1 Chebyshev-Collocation Method

The collocation is a weighted residual method used to approximate the solutions of a differential equation

$$L[u(\eta)]=f(\eta) \tag{20}$$

by starting with an initial approximate solution

$$u_N(\eta)=\sum_{k=0}^{N}c_k\phi_k(\eta), \tag{21}$$

where ϕ_k are the basis functions and c_k are unknown coefficients to be determined (Gebril et al., 2024). The residual is defined as

$$R(\eta)=L[u_N(\eta)]-f(\eta) \tag{22}$$

The next step is to find $N+1$ collocation points η_k, ($k=0,1,\cdots,N$) and ensure that the residual is zero at the the collocation points, so that

$$R(\eta_k)=0,\ \text{for } k=0,1,\cdots,N. \tag{23}$$

We are therefore required to solve the $N+1$ equations for the $N+1$ unknown coefficients c_k. By choosing the basis function ϕ_k as the Chebyshev polynomials, the method is referred to as Chebyshev-collocation method.
The Chebyshev polynomials $T_n(\xi)$ of the first kind are defined as

$$T_n(\xi)=\cos(n\arccos\xi) \tag{24}$$

over the interval $[-1,1]$ (Cevik et al., 2025). The polynomials are orthogonal with weight function

$$w(\xi)=\frac{1}{\sqrt{1-\xi^2}} \tag{25}$$

so that

$$\int_{-1}^{1}\frac{T_mT_n}{\sqrt{1-\xi^2}}d\xi=\begin{cases}\frac{\pi}{2} & n=m\neq 0\\ \pi & n=m=0\\ 0 & n\neq m\end{cases}. \tag{26}$$

The polynomials can be obtained from the recursive relation

$$T_{n+1}=2\xi T_n-T_{n-1} \tag{27}$$

and the roots of the the polynomial are

$$\xi_k=\cos\left(\frac{2k-1}{2n}\pi\right),\ k=1,2,\cdots,n. \tag{28}$$

and the derivative is

$$T_n'=\frac{n\sin(n\arccos\xi)}{\sqrt{1-\xi^2}}$$

Evaluating the polynomials at the end points $\xi=\pm1$, we have

$$T_n(-1)=\cos(n\arccos(-1))=\cos(n\pi)=(-1)^n,$$
$$T_n(1)=\cos(n\arccos(1))=\cos(n\times 0)=1,$$
$$\lim_{\xi\to1}T_n'=n^2,\ \lim_{\xi\to-1}T_n'=(-1)^{n+1}n^2.$$

3.2 Transformation of domain

The domain $\xi\in[-1,1]$ can be transformed into $\eta\in[0,L]$ using the transformation

$$\xi=\frac{2}{L}\eta-1,$$

so that the Chebyshev polynomials is evaluated for

$$T_n(\xi)=T_n\left(\frac{2}{L}\eta-1\right).$$

Evaluating the polynomials and their first derivatives at the end points $\eta=0,L$, we have

$$T_n(0)=(-1)^n,\ T_n(L)=1,$$
$$\lim_{\xi\to1}T_n'=n^2,\ \lim_{\xi\to-1}T_n'=(-1)^{n+1}n^2.$$

IV. Solution to the Model

Assume solutions of the form

$$f=\sum_{k=0}^{n}a_kT_k,\ \Theta=\sum_{k=0}^{n}b_kT_k,\ \Phi=\sum_{k=0}^{n}c_kT_k,$$

International Journal of Recent Development in Engineering and Technology
Website: www.ijrdet.com (ISSN 2347-6435 (Online) Volume 15, Issue 03, March 2026)

where T_k are the Chebyshev basis functions. This means there are

$$(n+1)+(m+1)+(m+1)=n+2m+3$$

coefficients to solve for. We therefore need a total of $n+2m+3$ equations. Since there are 7 boundary conditions, and then only $n+2m-4$ equations are needed. To get $n+2m-4$ collocation points from 3 equations, then $n+2m-4$ needs to be a product of 3. The easiest choice for n and m is to set $m=n-1$, so that

$$n+2m-4=n+2(n-1)-4=3n-6=3(n-1).$$

The Chebyshev collocation points are obtained using the formula

$$\xi_j=\cos\left(\frac{j\pi}{n-1}\right),\ j=0,\cdots,n-1$$

.

The internal nodes among the collocation points are picked so that we have a total of $n-2$ collocation points.

Substituting the series of equation (29) into equations (14) - (16), we have

$$\sum_{k=3}^{n}a_k\left[T_k'''+\left(1-\frac{(q+2)\delta^2}{3}\left(\sum_{j=2}^{n}a_kT_k''\right)^2\right)q\varepsilon T_k'''\left(\sqrt{2}\delta\sum_{j=2}^{n}a_kT_k''\right)^{q-1}-KT_k'-\sum_{j=1}^{n}a_jT_j'T_k'+\sum_{j=2}^{n}a_jT_kT_j''\right]-K\sum_{k=1}^{2}a_kT_k'-\sum_{k=1}^{2}\left(a_k\sum_{j=1}^{n}a_jT_j'T_k'\right)+\sum_{k=0}^{2}a_k\left(\sum_{j=2}^{n}a_jT_kT_j''\right)=0, \quad (30)$$

$$\sum_{k=2}^{m}\left[b_kT_k''+Pra_k\left(\sum_{j=1}^{m}b_jT_j'T_k\right)\right]+Pr\sum_{k=0}^{1}a_k\left(\sum_{j=1}^{m}b_jT_j'T_k\right)=0 \quad (31)$$

$$\sum_{k=2}^{m}\left[c_kT_k''+Sca_k\left(\sum_{j=1}^{m}c_jT_j'T_k\right)\right]+Sc\sum_{k=0}^{1}a_k\left(\sum_{j=1}^{m}c_jT_j'T_k\right)=0. \quad (32)$$

and equation (17) becomes

$$\sum_{k=0}^{n}(-1)^{k+1}k^2a_k=1,\ \sum_{k=0}^{n}(-1)^ka_k=0,\ \sum_{k=0}^{m}(-1)^kb_k=0,\ \sum_{k=0}^{m}(-1)^kc_k=0. \quad (33)$$

$$\sum_{k=0}^{n}k^2a_k=0,\ \sum_{k=0}^{m}b_k=1,\ \sum_{k=0}^{m}c_k=1. \quad (34)$$

Evaluating equations (30 - 32) at the $n-2$ collocation points means we are required to solve the system of non-linear equations;

$$\left\{\sum_{k=3}^{n}a_k\left[T_k'''+\left(1-\frac{(q+2)\delta^2}{3}\left(\sum_{j=2}^{n}a_kT_k''\right)^2\right)q\varepsilon T_k'''\left(\sqrt{2}\delta\sum_{j=2}^{n}a_kT_k''\right)^{q-1}-KT_k'-\sum_{j=1}^{n}a_jT_j'T_k'+\sum_{j=2}^{n}a_jT_kT_j''\right]-K\sum_{k=1}^{2}a_kT_k'-\sum_{k=1}^{2}\left(a_k\sum_{j=1}^{n}a_jT_j'T_k'\right)+\sum_{k=0}^{2}a_k\left(\sum_{j=2}^{n}a_jT_kT_j''\right)\right\}\Bigg|_{(\xi=\xi_p)}=0, \quad (35)$$

$$\sum_{k=2}^{m}\left[b_kT_k''+Pra_k\left(\sum_{j=1}^{m}b_jT_j'T_k\right)\right]+Pr\sum_{k=0}^{1}a_k\left(\sum_{j=1}^{m}b_jT_j'T_k\right)=0\Bigg|_{(\xi=\xi_p)}=0 \quad (36)$$

$$\sum_{k=2}^{m}\left[c_kT_k''+Sca_k\left(\sum_{j=1}^{m}c_jT_j'T_k\right)\right]+Sc\sum_{k=0}^{1}a_k\left(\sum_{j=1}^{m}c_jT_j'T_k\right)=0.\Bigg|_{(\xi=\xi_p)}=0. \quad (37)$$

$$\sum_{k=0}^{n}(-1)^{k+1}k^2a_k=1,\ \sum_{k=0}^{n}(-1)^ka_k=0,\ \sum_{k=0}^{m}(-1)^kb_k=0,\ \sum_{k=0}^{m}(-1)^kc_k=0. \quad (38)$$

$$\sum_{k=0}^{n}k^2a_k=0,\ \sum_{k=0}^{m}b_k=1,\ \sum_{k=0}^{m}c_k=1. \quad (39)$$

where $p=1,\cdots,n-2$. Hence, we have a total of $3(n-2)+7=3n+1$ equations to solve. Recall that there are $n+1$ coefficients $a_k,(k=0,\cdots,n)$, and there are n coefficients b_k and n coefficients c_k since $k=0,\cdots,n-1$. The total number of coefficients totals to

$$n+1+n+n=3n+1.$$

At this point, the number of equations tally with the number of the unknown and the equations can therefore be solved using the Newton's method.

V. Numerical Experiment

To validate the numerical method adopted in this study, consider the case where $q=1$, then equation (14), (15), and (16) reduce to

$$\left(1+\varepsilon\left(1-\delta^2\left(\frac{d^2f}{d\eta^2}\right)^2\right)\right)\frac{d^3f}{d\eta^3}-K\frac{df}{d\eta}-\left(\frac{df}{d\eta}\right)^2+f\frac{d^2f}{d\eta^2}=0 \quad (40)$$

$$\frac{d^2\Theta}{d\eta^2}+Prf\frac{d\Theta}{d\eta}=0, \quad (41)$$

$$\frac{d^2\Phi}{d\eta^2}+Scf\frac{d\Phi}{d\eta}=0. \quad (42)$$

Taking the values of parameters as $K=1$, $\varepsilon=0.5$, $\delta=0.1$, $Pr=0.72$, and $Sc=0.6$, then the equation further simplifies to

$$\left(1+0.5\left(1-0.01\left(\frac{d^2f}{d\eta^2}\right)^2\right)\right)\frac{d^3f}{d\eta^3}-\frac{df}{d\eta}-\left(\frac{df}{d\eta}\right)^2+f\frac{d^2f}{d\eta^2}=0$$

$$\frac{d^2\Theta}{d\eta^2}+0.72f\frac{d\Theta}{d\eta}=0,$$

$$\frac{d^2\Phi}{d\eta^2}+0.6f\frac{d\Phi}{d\eta}=0.$$

,

International Journal of Recent Development in Engineering and Technology
Website: www.ijrdet.com (ISSN 2347-6435 (Online) Volume 15, Issue 03, March 2026)

Consider $n = 3$, then the collocating polynomials are

$$f = a_0T_0 + a_1T_1 + a_2T_2 + a_3T_3, \quad (43)$$
$$\Theta = b_0T_0 + b_1T_1 + b_2T_2, \quad (44)$$
$$\Phi = c_0T_0 + c_1T_1 + c_2T_2. \quad (45)$$

Substituting T_0, T_1, T_2, and T_3, the equations become

$$\begin{aligned}&0.36a_0b_1 - 0.36a_1b_1 + 0.36a_2b_1 - 0.36a_3b_1 + b_2 - 1.44a_0b_2 + 1.44a_1b_2 - 1.44a_2b_2 + 1.44a_3b_2\\&+ (0.18a_1b_1 - 0.72a_2b_1 + 1.62a_3b_1 + 0.72a_0b_2 - 1.44a_1b_2 + 3.6a_2b_2 - 7.2a_3b_2)\,\eta\\&+ (0.18a_2b_1 - 1.08a_3b_1 + 0.36a_1b_2 - 2.16a_2b_2 + 7.56a_3b_2)\,\eta^2\\&+ (0.18a_3b_1 + 0.36a_2b_2 - 2.88a_3b_2)\,\eta^3 + 0.36a_3b_2\eta^4 = 0 \quad (46)\end{aligned}$$

$$\begin{aligned}&0.3a_0c_1 - 0.3a_1c_1 + 0.3a_2c_1 - 0.3a_3c_1 + c_2 - 1.2a_0c_2 + 1.2a_1c_2 - 1.2a_2c_2 + 1.2a_3c_2\\&+ (0.1a_1c_1 - 0.6a_2c_1 + 1.35a_3c_1 + 0.6a_0c_2 - 1.2a_1c_2 + 3a_2c_2 - 6a_3c_2)\,\eta\\&+ (0.15a_2c_1 - 0.9a_3c_1 + 0.3a_1c_2 - 1.8a_2c_2 + 6.3a_3c_2)\,\eta^2\\&+ (0.15a_3c_1 + 0.3a_2c_2 - 2.4a_3c_2)\,\eta^3 + 0.3a_3c_2\eta^4 = 0 \quad (47)\end{aligned}$$

Consider $n = 3$, then the collocating polynomials are

and the boundary conditions become,

$$a_0 - a_1 + a_2 - a_3 = 0, \quad a_1 - 4a_2 + 9a_3 = 2, \quad b_0 - b_1 + b_2 = 0$$
$$c_0 - c_1 + c_2 = 0, \quad a_1 + 4a_2 + 9a_3 = 0, \quad b_0 + b_1 + b_2 = 1, \quad c_0 + c_1 + c_2 = 1$$

The collocation points are chosen as the interior points among

$\xi_0 = -1$, $\xi_1 = 0$, $\xi_2 = -1$.

Hence, the equations to solve are

The solution are obtained using MATHEMATICA as

$f = 0.0293 - 0.2596\eta + 0.7772\eta^2 + 0.0383\eta^3$, $\theta = 0.587015\eta - 0.0842537\eta^2$, $\phi = 0.530846\eta - 0.0702114\eta^2$.

Validation of Results

The results from the Chebyshev-collocation method is compared with the results from MATLAB bvp4c for validation. For the sake of comparison, the following values are chosen for the parameters;

$q = 1$; $Pr = 0.72$; $\varepsilon = 0.5$; $\delta = 0.1$; $K = 1$; $Sc = 0.6$; $\eta_\infty = 5$.

The Chebyshev-collocation method is solved for increasing number of terms n and the results are compared at each truncation and the comparison is shown in table (1). The table reveals that the results get better as n gets larger. From the table, the error becomes insignificant at $n \geq 11$. Hence, it can be concluded that method of solution is admissible for the current problem.

Table 1:
Validation of Results

n	C_f			Nu			Sh		
	bvp4c	present	Error	Nu	present	Error	Sh	present	Error
3	-1.15609	-1.07034	8.57e-02	0.45755	0.48654	2.90e-02	0.41255	0.43378	2.12e-02
4	-1.15609	-1.13154	2.46e-02	0.45755	0.46822	1.07e-02	0.41255	0.41980	7.25e-03
5	-1.15609	-1.15009	6.01e-03	0.45755	0.45981	2.26e-03	0.41255	0.41401	1.45e-03
6	-1.15609	-1.15479	1.30e-03	0.45755	0.45753	1.53e-05	0.41255	0.41255	6.25e-06
7	-1.15609	-1.15583	2.66e-04	0.45755	0.45730	2.53e-04	0.41255	0.41241	1.49e-04
8	-1.15609	-1.15604	5.51e-05	0.45755	0.45742	1.30e-04	0.41255	0.41248	7.47e-05
9	-1.15609	-1.15608	1.25e-05	0.45755	0.45751	4.16e-05	0.41255	0.41253	2.37e-05
10	-1.15609	-1.15609	3.21e-06	0.45755	0.45754	8.84e-06	0.41255	0.41255	5.13e-06
11	-1.15609	-1.15609	8.86e-07	0.45755	0.45755	6.45e-07	0.41255	0.41255	5.00e-07
12	-1.15609	-1.15609	2.54e-07	0.45755	0.45755	4.51e-07	0.41255	0.41255	1.77e-07

VI. Analysis And Discussion Of Results

The results obtained from the numerical solution are analysed and discussed in this section. The results are analysed in relation to existing academic literature to assess their conformity with theoretical expectations, and highlight areas of divergence that warrant additional inquiry.

Figures (2 - 4) illustrate the effect of Coriolis force on the flow variables. The numerical results plotted in Figure (2) reveals that Coriolis force K reduces velocity. This result is theoretically expected and aligns well with classical rotating flow dynamics. The Coriolis force arises due to the rotation of the frame, and introduces an apparent inertial force that acts perpendicular to the direction of motion. This force inhibits the forward motion of fluid particles, resulting in a reduced axial velocity. This outcome aligns with the outcome of Oke (2021) who also reported a noticeable reduction in axial velocities as Coriolis force increased. As Coriolis effects increases, the centrifugal and rotational inertial forces acting on fluid elements increase which consequently opposes both the primary stretching and the convective forces driving the flow. The momentum boundary layer thins out and the flow velocity is hindered, thereby reducing the velocity.

Figure (3) illustrates the response of temperature to Coriolis force. The influence of Coriolis force is also observed on the thermal characteristics of a Modified Eyring-Powell (MEP) fluid. The results of this study indicate that increasing the Coriolis parameter leads to a decrease in temperature within the boundary layer. As the Coriolis force parameter represents the influence of rotation on the flow field, this observation stands in contrast to Oke (2021) who reported a temperature increase under similar conditions. However, the divergence in result can be traced to the choice of the deformation parameter $q = 1$ which indicate a distinct fluid rheology as noted by Oke (2022). Oke (2022) noted that the fluid is shear-thickening for odd values of q while even values of q represent shear thinning case.

International Journal of Recent Development in Engineering and Technology
Website: www.ijrdet.com (ISSN 2347-6435 (Online) Volume 15, Issue 03, March 2026)

In the current study where $q = 1$, a shear-thickening fluid is therefore under consideration. Hence, the cooling effect observed in Figure (3) is consistent with a shear-thickening MEP fluid. In such a rheological flow, amplified rotational resistance acts as a thermal insulator, preventing the thermal energy from diffusing significantly within the fluid domain. The concentration field is the distribution of species within the flow domain and it determined by both the motion of the fluid and the mass diffusivity.

Figure (4) demonstrates that as the rotational parameter K increases, the concentration profile decreases, indicating a dilution of species concentration within the boundary layer. Since the species concentration are advected by the velocity field and diffused by molecular or turbulent processes. Thus, any suppression of velocity due to increasing directly impacts the advective capacity of the flow to transport species away from or along the surface.

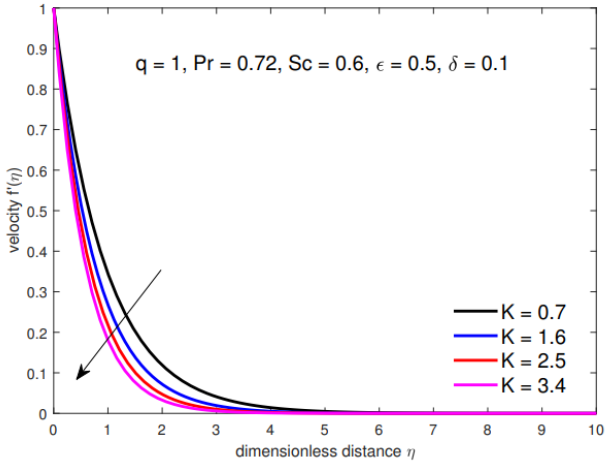

Figure II: Velocity with increasing *K*

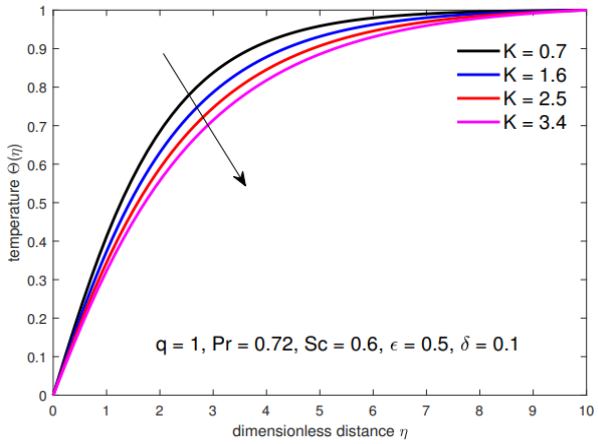

Figure III: Temperature with increasing *K*

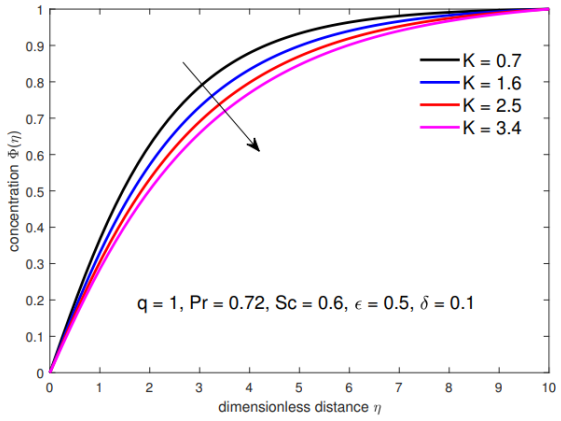

Figure IV: Concentration with increasing *K*

The parameter ϵ denotes material parameter which characterizes the extent of deviation from Newtonian behaviour. It governs the degree of elastic resistance or strain-rate sensitivity in the fluid. Figures (5 - 7) show the response of the flow variable to the Eyring-Powell parameter. The velocity increases with increasing Eyring-Powell fluid parameter as shown in Figure (5). The parameter amplifies the impact of the non-Newtonian term in the constitutive equation. This term governs shear-thickening behaviour, meaning that the fluid resists motion more as the shear rate increases, especially near the wall. Consequently, an increased axial flow is experiences due to a steeper pressure gradient or stretching.

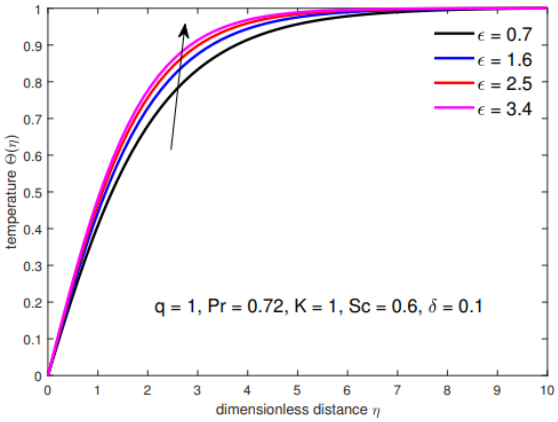

Figure V: Velocity with increasing ϵ

Figure (6) reveals that the temperature also rises as the material parameter increases. As the parameter increases, the fluid becomes more sensitive to shear, which raises the effective viscosity near the wall, dampens the convective transport of heat, and intensifies viscous dissipation.

International Journal of Recent Development in Engineering and Technology
Website: www.ijrdet.com (ISSN 2347-6435 (Online) Volume 15, Issue 03, March 2026)

The cumulative effect is an accumulation of thermal energy near the wall, manifesting as a rise in the temperature profile throughout the domain. The fluid becomes sensitive to shear as ϵ increases and the effective viscosity near the wall also increases. The convective thermal transport dampens and viscous dissipation intensifies and the cumulative effect is an accumulation of thermal energy near the wall, manifesting as a rise in the temperature profile throughout the domain.

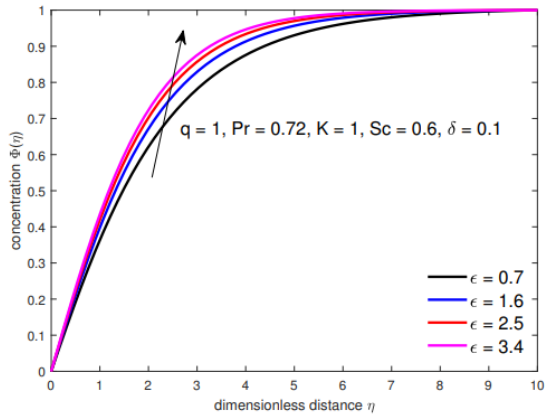

Figure VI: Temperature with increasing ϵ

Figure (7) shows the response of concentration to the Eyring-Powell fluid parameter. The concentration profile is governed by a balance between advection and diffusion, which are both affected by the parameter. This diminished convective mixing leads to retention of species near the surface, thus raising the concentration within the boundary layer.

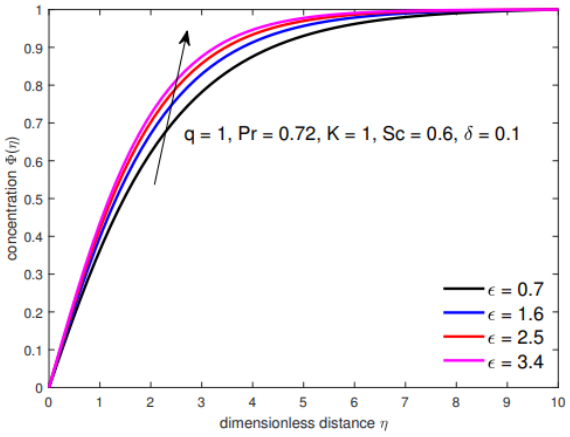

Figure VII: Concentration with increasing ϵ

The Prandtl number (Pr) is a dimensionless parameter that quantifies the relative thickness of the momentum and thermal boundary layers. Increasing Prandtl number implies decreasing thermal diffusivity relative to momentum, resulting in thinner thermal boundary layers. Figure (8) shows that fluid temperature increases with Prandtl number. As the thermal diffusivity decreases, the boundary becomes better at retaining heat more effectively because it diffuses slowly into the bulk fluid. Consequently, the near-wall fluid experiences thermal accumulation, leading to higher local temperatures.

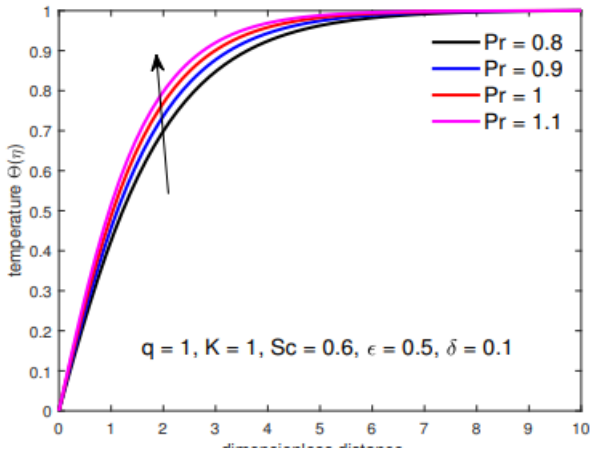

Figure IX: Temperature with increasing *Pr*

The Schmidt number (Sc) is the ratio of momentum diffusivity to mass diffusivity. High Schmidt number implies low mass diffusivity and species diffuse slowly compared to momentum. Figure (9) shows that increasing the Schmidt number leads to an increase in the concentration profile within the boundary layer of the Modified Eyring-Powell fluid over a rotating surface.

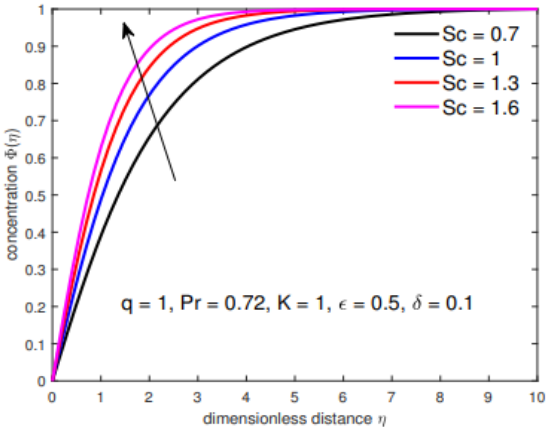

Figure 9: Concentration with increasing *Sc*

International Journal of Recent Development in Engineering and Technology
Website: www.ijrdet.com (ISSN 2347-6435 (Online) Volume 15, Issue 03, March 2026)

VII. Conclusion

This study analyses the heat and mass transfer characteristics in the flow of Modified Eyring-Powell (MEP) fluid over a rotating surface. The study has been able to achieve the four specific objectives. The first objective was achieved through an empirical derivation of the equations governing the boundary layer flow of the MEP fluid. The model incorporated concentration equation and the Coriolis force arising from the rotating system. The second objective was achieved by applying the similarity transformations to reduce the partial differential equations into a system of dimensionless non-linear ordinary differential equations. The third objective was achieved by employing the Chebyshev-collocation method and the result was validated against MATLAB's bvp4c solver to confirm the accuracy and convergence of the method. The numerical solution from the Chebyshev-collocation method convergence to the solution from the bvp4c solver for $n \geq 11$. The outcomes of the study revealed that; steps required to achieve the general objective of this study are as follows;

i. Coriolis force suppresses velocity, temperature, and concentration in modified Eyring-Powell fluid.
ii. Eyring-Powell fluid parameter reinforces velocity, temperature, and concentration.
iii. Prandtl number increases temperature and Schmidt number increases concentration.

VIII. Recommendations

This study has considered heat and mass transfer characteristics of Modified Eyring-Powell fluid over a rotating surface and the following recommendations are proposed for further research and practical application;

i. The choice of $q = 1$ restricts our study the shear-thickening behaviour of the MEP fluid. Future work can explore other values of q, to generalise the findings across a wider class of non-Newtonian fluids.
ii. To adapt this study to polymer processing, bioreactors, chemical vapour deposition and thermal insulation, the study can incorporate chemically reactions, magnetohydrodynamic forces and thermal radiation in 3D porous media.
iii. The bifurcation analysis, perturbation response, and critical thresholds for the flow transition is recommended for further studies.

REFERENCES

[1] Aaqil, M., Peng, C., Kamal, A., Nawaz, T., Zhang, F., and Gong, J. (2023). Tea Harvesting and Processing Techniques and Its Effect on Phytochemical Profile and Final Quality of Black Tea: A Review. *Foods*, 12(24):4467.

[2] Abegunrin, O. A., Animasaun, I. L., and Sandeep, N. (2017). Insight into the boundary layer flow of non-Newtonian Eyring-Powell fluid due to catalytic surface reaction on an upper horizontal surface of a paraboloid of revolution. *Alexandria Engineering Journal*, pages 1–10.

[3] Anjum, N., Khan, W., Hobiny, A., Azam, M., Waqas, M., and Irfan, M. (2022). Numerical analysis for thermal performance of modified eyring powell nanofluid flow subject to activation energy and bioconvection dynamic. *Case Studies in Thermal Engineering*, 39:102427.

[4] Anjum, N., Khan, W. A., Ali, M., and Hussain, I. (2023). Impact of tiny nanoparticles on generalized eyring-powell liquid subject to activation energy. *International Journal of Modern Physics B*, 38(14).

[5] Cevik, M., Savasaneril, N. B., and Sezer, M. (2025). A Review of Polynomial Matrix Collocation Methods in Engineering and Scientific Applications. *Archives of Computational Methods in Engineering*.

[6] Gebril, E., El-Azab, M., and Sameeh, M. (2024). Chebyshev collocation method for fractional Newell-WhiteheadSegel equation. *Alexandria Engineering Journal*, 87:39–46.

[7] Junaid, M. S., Aslam, M. N., Ali, A., Ali, H., Amjad, M., Shah, N. A., and Alshehri, M. (2023). Analysis of modified eyring-powell fluid under magnetic dipole effect over a stretching flat plate. *The European Physical Journal Plus*, 138(9).

[8] Khan, W. A. (2023). Dynamics of gyrotactic microorganisms for modified eyring powell nanofluid flow with bioconvection and nonlinear radiation aspects. *Waves in Random and Complex Media*, pages 1–11.

[9] Khan, W. A. and Uddin, M. J. (2023). Nano-bioconvective anisotropic slip flow in anisotropic porous medium with coriolis force effects. *Heat Transfer*, 53(2):558–583.

[10] Koriko, O. K., Adegbie, K. S., Oke, A. S., and Animasaun, I. L. (2020). Exploration of Coriolis force on motion of air over the upper horizontal surface of a paraboloid of revolution. *Physica Scripta*, 95(3):035210.

[11] Kumar, B. and Srinivas, S. (2020). Unsteady Hydromagnetic Flow of Eyring-Powell Nanofluid over an Inclined Permeable Stretching Sheet with Joule Heating and Thermal Radiation. *Journal of Applied and Computational Mechanics*, 6(2):259–270.

[12] Lou, Q., Ali, B., Rehman, S. U., Habib, D., Abdal, S., Shah, N. A., and Chung, J. D. (2022). Micropolar dusty fluid: Coriolis force effects on dynamics of mhd rotating fluid when lorentz force is significant. *Mathematics*, 10(15):2630.

[13] Oke, A. (2021). Coriolis effects on mhd flow of mep fluid over a non-uniform surface in the presence of thermal radiation. *International Communications in Heat and Mass Transfer*, 129:105695.

[14] Oke, A. (2022). Theoretical analysis of modified eyring powell fluid flow. *Journal of the Taiwan Institute of Chemical Engineers*, 132:104152.

[15] Oke, A. S., Eyinla, T., and Juma, B. A. (2023). Effect of coriolis force on modified eyring powell fluid flow. *Journal of Engineering Research and Reports*, 24(4):26–34.

[16] Oke, A. S. and Mutuku, W. N. (2021). Significance of viscous dissipation on MHD Eyring-Powell flow past a convectively heated stretching sheet. *Pramana*, 95(4).

[17] Patel, M. and Timol, M. G. (2009). Numerical treatment of Powell-Eyring fluid flow using Method of Satisfaction of Asymptotic Boundary Conditions (MSABC). *Applied Numerical Mathematics*, 59:2584–2592.

[18] Rahimi, J., Ganji, D. D., Khaki, M., and Hosseinzadeh, K. (2017). Solution of the boundary layer flow of an Eyring-Powell non-Newtonian fluid over a linear stretching sheet by collocation method. *Alexandria Engineering Journal*, pages 622–627.

[19] Rathnayake, C., Griffith, G., Sinnett, A., Malcolm, B., and Farquharson, B. (2023). Developing an equilibrium displacement model of the sri lankan tea industry.

[20] Siddiqui, A. M., Haroon, T., and Zeb, M. (2014). Analysis of Eyring-Powell Fluid in Helical Screw Rheometer. *The Scientific World Journal*, 2014:1–14.